5.53 — polimery

Andrzej Wasiak

APPLICATION OF SCATTERING METHODS TO THE STUDIES OF THE STRUCTURE OF POLYMER BLENDS

13/1984

WARSZAWA 1984

ISSN 0208-5658

Praca wpłynęła do Redakcji dnia 10 lutego 1984 r.

IPPT PAN

Na prawach rękopisu

Instytut Podstawowych Problemów Techniki PAN
Nakład 140 egz. Ark.wyd.2,5. Ark.druk. 3,75.
Oddano do drukarni w marcu 1984 r.
Nr zamówienia 201/84.

Warszawska Drukarnia Naukowa, Warszawa,
ul.Śniadeckich 8

Andrzej Wasiak
Pracownia Fizyki Polimerów
IPPT PAN, Warszawa

APPLICATION OF SCATTERING METHODS TO THE STUDIES OF THE STRUCTURE OF POLYMER BLENDS

INTRODUCTION

Blending of various polymers appears to be important and effective way of modification of properties of polymeric materials. It is worth to note that not only chemical composition of constituents but also physical structure (morphology) of the blend determines its final properties. This situation produces need for appropriate methods for characterization of the morphology as well as need for studies of the effects of morphology on the physical properties of blends. Qualitative, and some quantitative informations can be obtained from direct observations by means of optical and electron microscopy, the other more sophisticated data are available from experiments involving scattering phenomena.

The aim of the present paper is to review possible applications of scattering methods using different types of radiation towards the studies of the structure of polymer blends.

SCATTERING PHENOMENA

When any electromagnetic or corpuscular radiation passes through inhomogeneous material system, the interaction between inhomogeneities and the radiation produces spreading of the radiation in a certain angular range quite apart from the

direction of the incident beam. This phenomenon is known as scattering of the radiation. One can describe the amplitude of the scattered wave, A(s) using following formula[1]

$$A(\underset{\sim}{s}) = A_o \sum_n^N f_n \exp[ik(\underset{\sim}{r}_n \cdot \underset{\sim}{s})] \qquad (1)$$

where A_o - is amplitude of incident radiation, $k = 2\pi/\lambda$ is constant for a given wavelength, λ, of the radiation, and $\underset{\sim}{s} = \underset{\sim}{i}_o - \underset{\sim}{i}_s$ is a scattering vector defined by unit vectors $\underset{\sim}{i}_o$ and $\underset{\sim}{i}_s$ directed towards directions of incident and scattered beams (cf. Fig.1). The magnitude of this vector is

$$|s| = 2 \sin(\Theta/2) \qquad (2)$$

Another variable

$$h = k|s| = \frac{4\pi}{\lambda} \sin(\Theta/2) \qquad (3)$$

is also frequently used in the description of scattering. An angle, Θ, is the angle between directions of incident and scattered beams.

As it is seen in formula (1), an amplitude of scattered wave in particular direction depends on scattering power, f_n, of each of N individual elements as well as on the positions, $\underset{\sim}{r}_n$, of the elements with respect to arbitrarily choosen coordinate system. The set of N values of scattering power, f_n, and coordinates, $\underset{\sim}{r}_n$, can be considered as the description of the structure of a given scattering body. Studies on the angular distribution of radiation amplitude might therefore provide the details of the structure of a material. It has to be noted here that the structure of a real system is usually

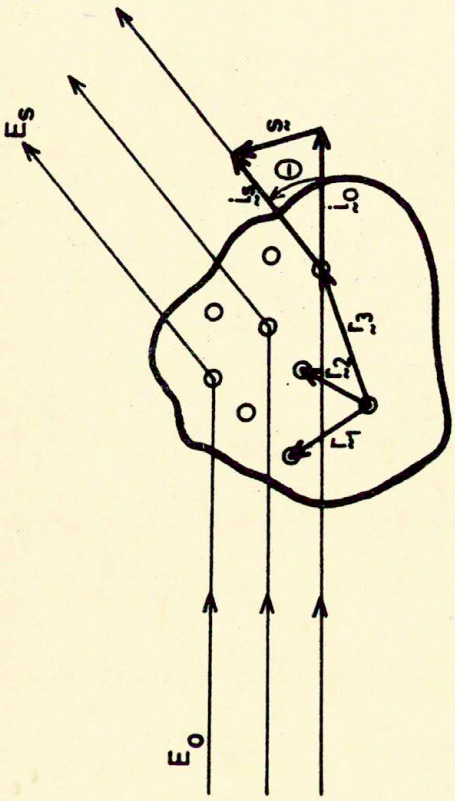

Fig. 1. Scattering of the radiation on inhomogeneous body.

Table 1

Wavelengths of various radiations being used for structural studies

radiation	range of λ (A^o)
X-Rays	0.5 - 2.5
electrons	0.1 - 1.0
neutrons	1.0 - 15
light	4000 - 6000
microwaves	10^7 - 10^8

quite complicated, and reveals a number of levels differing in both: the range of characteristic distances, and the scattering power of objects that can be considered as individual structural elements (e.g. atoms, molecules, crystals, spherulites etc.). One can therefore think about a structure of individual molecule in terms of interatomic distances, and scattering powers of individual atoms, or about structure of condensed matter in terms of intermolecular distances and scattering powers of individual molecules. In the same manner higher levels of structure can be described by means of interlamellar or interspherulitic distances and scattering powers of lamellae or spherulites, as well as in terms of distances between domains together with scattering power of the individual domain in a case of incompatible polymer mixtures or block copolymers.

Distances between scattering centers might substantially differ in various levels of the structure. This affects the behavior of radiations differing in wavelength. The ranges of wavelength of various radiations are summarized in Table I. Using the variable, h, defined in eq.(3) one can discuss the effect of characteristic distance of the structure on the scattering phenomena. According to eq.(1), the effects of particular distance, r_n, for various radiations can be expected at scattering angles giving the same values of $h = ks$. In Table 2 a comparison of scattering angles corresponding to the same, h, for visible light and for X-Rays are shown together with the comparison of values, h, corresponding to the same angle Θ. It is easy to recognize that the same distance produces an effect at quite large angle in the case of visible light, whereas equivalent effect will be observed at very small angle in the case of X-Rays. Consequently, the effect observed at the same angle corresponds to much bigger distances in a structure studied by means of light scattering than in a case of investigation performed by means of X-Rays.

Scattering power of an individual element depends not only upon its physical constitution, but also appears to be dependent on the type of incident radiation. A classical example can be given by comparison of scattering power of

Table 2

Effect of wavelength on scattering phenomena

radiation	wavelength (A^o)	scattering angle (deg)	h (A^{o-1})	h^{-1} (A^o)
light	6000	45	$8.015 \cdot 10^{-4}$	$1.248 \cdot 10^{3}$
X-Rays	1.5	$1.1 \cdot 10^{-2}$	$8.015 \cdot 10^{-4}$	$1.248 \cdot 10^{3}$
X-Rays	1.5	45	3.206	0.312

various atoms towards X-Rays and Neutrons. In a case of X-Rays a single electron plays important role as a scatterer. Therefore scattering power of an atom with respect to X-Rays strongly depends upon atomic number of an element (number of electrons in the atom). Moreover, since electrons are located on the outer part of the atom forming the cloud of size comparable with wavelength of X-Rays, the interference takes place, causing fast decrease of scattering intensity with an increase of scattering angle, Θ (an increase of $\underset{\sim}{s}$).

On the contrary, neutrons are scattered by nuclei of atoms. In consequence the scattering power of an atom is almost independent of the angle, Θ (cf. Fig.2).

Also the scattering power of atoms of various elements only slightly depends on their atomic numbers. As shown in Fig.3, the dependence is not monotonic but show substantial jumps resulting from effects caused by differences in structure of atomic nucleus. A classical example is seen in dramatic difference between scattering powers of hydrogen $f_H = -0.374 \cdot 10^{-12}$ cm, and deuterium $f_D = 0.667 \cdot 10^{-12}$ cm. This phenomenon found a number of important applications in the investigation of various details of crystal and molecular structure (including structure of polymers).

As it was mentioned, the equation (1) relates structural characteristics like coordinates, $\underset{\sim}{r}_n$ of the scattering centers, and their scattering powers, f_n, to amplitudes $A(s)$ of radiation scattered in various directions, $\underset{\sim}{s}$. Therefore, having known the angular distribution of scattered amplitude, one would attempt to determine the structure of the material. Unfortunately, this distribution is usually not accessible to measurements. Only intensities, being squares of the complex amplitudes, are measurable. Because of that, part of the information contained in the initial phases of complex amplitudes, is lost in the intensity measurements. Therefore, eq. (1) cannot be solved without any additional assumptions. Due to this, some indirect methods have to be used to determine the structure, e.g. one has to consider particular model to predict the intensity distribution. Comparison of this model-calculated intensity distribution with the measured one,

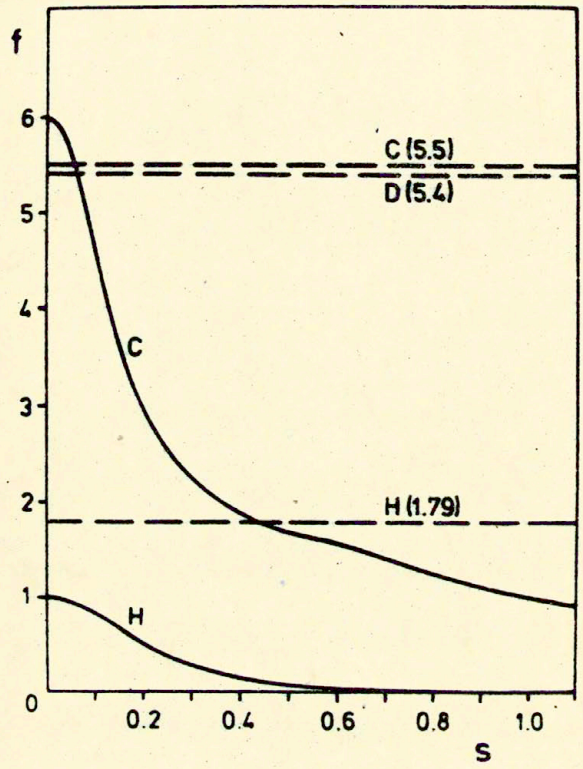

Fig. 2. Comparison of dependencies of scattering power of an atom upon the scattering angle, Θ, for the case of X-Ray and neutron radiation.

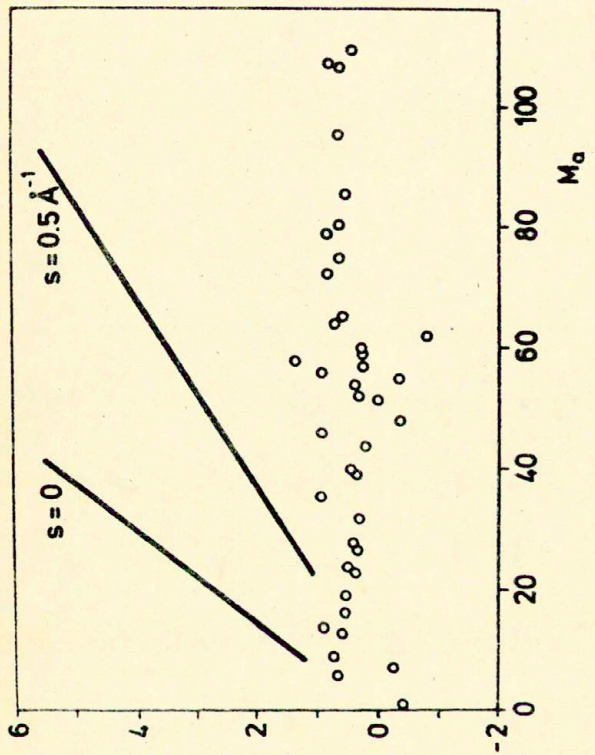

Fig. 3. Scattering power for X-Rays and neutrons as a function of atomic number.

becomes a basis for final conclusions. Frequently a number of competitive models can be proposed to explain the same intensity distribution. Selection between them can only be made basing on additional informations from another source.

A variety of approaches have been elaborated for studying the structure of materials by means of scattering techniques. Usually, they can be classified into few groups concerning investigations of:

1. individual particle,
2. dilute systems of particles,
3. concentrated system of particles,
4. ordered systems.

Some details of these approaches are reviewed in the following chapters of the paper.

SCATTERING BY VARIOUS OBJECTS

1. Individual Elements

One of the most important models for calculation of the intensity distribution of scattered radiation is a homogeneous sphere of radius R and scattering power, ϱ_s, embedded into homogeneous matrix of different scattering power, ϱ_o. The intensity distribution in such a case is represented by well known formula[1]

$$I(s) = K\, I_o\, V_s^2 (\varrho_s - \varrho_o)^2 [\Phi(u)]^2 \qquad (4)$$

where $u = hR$, V_s is volume of the sphere, and

$$\Phi(u) = \frac{3(\sin u - u\cos u)}{u^3} \qquad (5)$$

The shape of the function $[\Phi(u)]^2$ is shown in Fig.4.

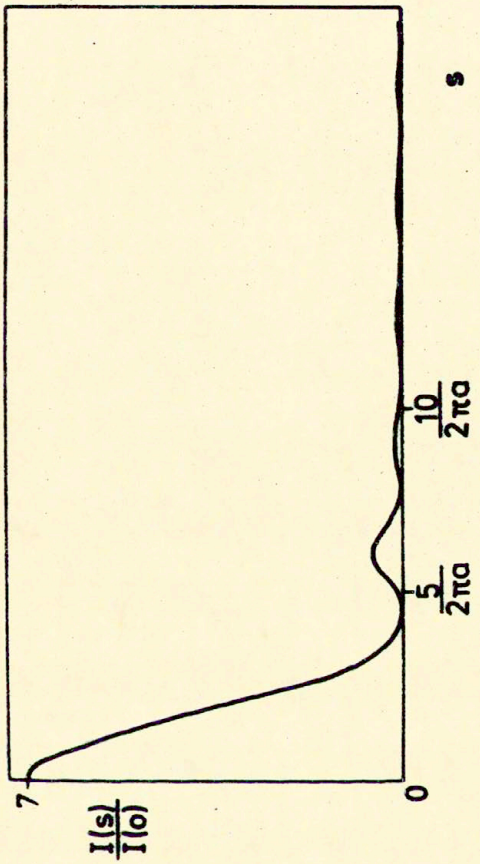

Fig. 4. Intensity distribution for a radiation scattered on homogeneous sphere.

Similar equations have been derived for ellipsoids[3], cylinders, and many other geometrical forms[2].

The eq.(4) may equally represent scattering of X-Rays on the particle of some uniform electron density, as well as scattering of neutrons arising from a spherical object of uniform atomic density or scattering of unpolarized light on a transparent sphere of one refractive index embedded into matrix of another refractive index.

Extension of this approach to the sphere of anisotropic scattering power, for example a spherulite with different radial and tangential polarizabilities, provides a number of expressions corresponding to various modes of polarization of the incident radiation and polarization of the observed component of scattered radiation. As an example for the case of H_V mode (polarization directions in polarizer and analyzer crossed) the expression assumes form[4,5]

$$\Phi_{HV}(u) = \frac{4\ \sin u - u\cos u - Si u}{u^3} \qquad (6)$$

Since this function reaches maximum at $u_{max} = 4.1$, the relation between angular position of the maximum of scattered light intensity, Θ_{max}, and spherulite radius, R, can be written in form

$$R = \frac{4.1\ \lambda}{4\pi\ \sin(\Theta_{max}/2)} \qquad (7)$$

where λ - is wavelength of light.

Similar approach have been applied to the individual macromolecule with gaussian segmental statistics, resulting in formula

$$I = I_o \frac{2}{V^2} \left\{ V - 1 + \exp(-V) \right\} \qquad (8)$$

where $V = h^2 R_g$

R_g - being the radius of gyration of the macromolecule.

ii. Dilute Systems

It is very rear case to observe the scattering on individual element alone. A number of systems, however, behave like a single element in the sense that the intensity distribution obtained from the system has the same form as corresponding one from the single element. This may happen when the distances between elements are much bigger then wavelength of the radiation, and consequently all elements scatter independently. In such a case the intensity scattered by the whole irradiated system is a sum of contributions, I_i, from individual particles. The resulting intensity, I, has the same form as I_i when the later are isotropic or in a case of non-isotropic contributions from the elements oriented in parallel. The angular distribution of intensity arising from randomly oriented non-isotropic elements is distorted with respect to an individual contribution and can be expressed as follows:

$$I(\Theta) = \frac{N}{4\pi} \int_0^{2\pi} I(\varphi, \Theta) \sin\varphi \, d\varphi \qquad (9)$$

where angle φ - represents the angle between the reciprocal vector giving contribution to the scattering and the reference direction (orientation axis), Θ - is the scattering angle, and N - the number of scattering elements. It has to be noted, however, that in some cases informations concerning the shape of scattering elements can be deducted from the measured average

intensity distribution, $I(\Theta)$ by appropriate application of Lorentz factors[7,8].

iii. Concentrated Systems of Scattering Centers

Substantial modification of the intensity distribution with respect to a distribution produced by an individual element, occurs when distances between elements are comparable to the wavelength of the radiation. In such a case, the interference of waves scattered by different elements play important role, determining the character of the intensity distribution. Therefore not only scattering power of individual element, but also mutual arrangement of scattering centers are responsible for the distribution of scattered intensity. Using this intensity distribution to the studies of the structure of the system, one meets a problem to distinguish properly between intra-, and interparticle contributions. Quite often, the knowledge of particle scattering coming from the studies on diluted systems of the same particles is extremely valuable.

In a case of liquid-like systems, in which no long-range order exist, a notion of correlation function prooved itself to be a description of structure, useful in developing mathematical relations between structure and scattered intensity distribution. This function is defined as follows[9]

$$\gamma(r) = \frac{\langle \eta_i \, \eta_j \rangle_r}{\bar{\eta}^2} \qquad (10)$$

where $\bar{\eta}^2 = (\varrho_i - \bar{\varrho})^2$ is mean square fluctuation of scattering power ϱ_i, η_i and η_j denote fluctuations occuring in points i, j, and separated by a distance, r. Since the product $\eta_i \, \eta_j$ assumes non-zero values only when simultaneously both η_i and η_j differ from zero, these non-zero values indicate the presence of fluctuations separate by particular distance. The product $\eta_i \, \eta_j$ averaged over all pairs of volume elements

separated by the same distance, r, is then a measure of probability of finding a pair of fluctuations separated by the distance, r. In other words, it indicates the probability of correlation between fluctuations separated by this distance.

The intensity of radiation scattered by an object, being related to the correlation function $\gamma(r)$ is given as

$$I(h) = K \eta^2 \int_0^\infty \gamma(r) \frac{\sin(hr)}{hr} r^2 dr \qquad (11)$$

where K - is constant dependent upon the character of the radiation used, and on some experimental conditions.

Function $\gamma(r)$ can be evaluated from experimental intensity distribution I(h) by an inverse Fourier transform. This approach have found many applications in various branches of structure analysis, like wide-, and small-angle X-Ray scattering[10,11], small-angle light scattering[12]. In the case of wide-angle X-Ray scattering observed from liquids, as well as from amorphous solid materials the idea of radial distribution function[13] is frequently used. This function, being analogous to above mentioned correlation function, also can be evaluated by means of inverse Fourier transform from the intensity distribution

$$4\pi r^2[\varrho(r) - \varrho_0] = \frac{2r}{\pi} \int_0^\infty h \frac{I(h) - I(\infty)}{I(\infty)} \sin hr \, dh \qquad (12)$$

The radial distribution function describes local packing of atoms in subsequent coordinate shells at radial distances, r, measured from any atom choosen as the origin. In recent years some interest was focused the application of this method to the studies of amorphous and semicrystalline polymers[14-17]. An

example of such analysis[17], made for poly(ethylene terephthalate) is shown in Fig.5.

An alternative approach, basing upon direct computation of scattered intensity from various models of the structure, is also offered. Examples of this approach are given in papers[18-20] for the case of SAXS, and papers[21-23] for the case of SALS.

Important results were obtained in[23] giving possibility for extensive analysis of H_V and V_V light scattering patterns in order to evaluate details of polymer morphology (cf. discussion in[24]). The resulting formulas for Rayleigh ratios in H_V and V_V polarization modes reads as follows

$$R_{HV}(\Theta,\mu) = K\varphi_s R_s^3(\alpha_t - \alpha_r)^2 \Phi_{HV}^2(h)\sin^2\mu \cos^2\mu[\chi(\Theta,\mu)F(\Theta,\mu)]_{HV}^{-1} \tag{13a}$$

$$R_{VV}(\Theta,\mu) = K B(\varphi_s)R_s^3\{(\alpha_t - \alpha_d)\Phi_{VV}(h) + (\alpha_r - \alpha_d)\Phi'_{VV}(h) + (\alpha_t - \alpha_r)\cos^2\mu \Phi_{HV}(h)\}^2[\chi(\Theta,\mu)F(\Theta,\mu)]^{-1} \tag{13b}$$

where constant $K = 192\pi^5/\lambda^4$, and φ_s is volume fraction of spherulites, $\chi(\Theta,\mu)$ is multiple scattering factor, $F(\Theta,\mu)$ is disorder correction factor. Scattering functions are expressed as

$$\Phi_{HV}(h) = \frac{4\sinh - h\cosh - Sih}{h^3} \tag{14a}$$

$$\Phi_{VV}(h) = \frac{2\sinh - h\cosh - Sih}{h^3} \tag{14b}$$

$$\Phi'_{VV}(h) = \frac{Sih - \sinh}{h^3} \tag{14c}$$

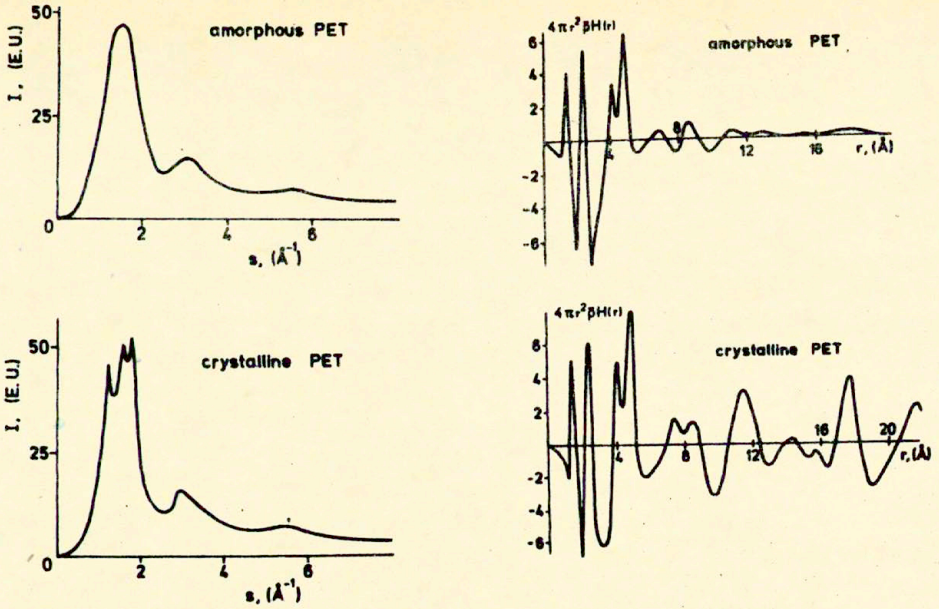

Fig. 5. X-Ray intensity distributions and corresponding radial distribution functions for amorphous and semicrystalline poly(ethylene terephthalate)

the average polarizability of the system assumes form

$$\alpha_d = [(\alpha_t + 2\alpha_r)/3]\varphi_s + \alpha_m(1 - \varphi_s) \qquad (15)$$

where α_r and α_t are radial and tangential polarizabilities of spherulite and α_m is polarizability of a medium surrounding the spherulite.

Analysis of H_V and V_V scattering modes gives not only the possibility to evaluate average spherulite radius R_s, but also enables deeper insight into the structure, through possible determination of polarizabilities of the spherulite α_r, α_t, and of the medium α_m.

iv. Ordered Systems

In many cases scattering elements are ordered. It means that subsequent elements have the same orientations with respect to an external coordinate system and that in relatively long rows chosen along various directions they are separated by the same distance characteristic for the particular direction. The best example of such long-distance order is crystal, which is built of atoms or molecules forming three--dimensional lattice. Similar objects, having one-, or two--dimensional order of molecular packing are also known. Higher levels of structure give other examples of superstructures containing ordered elements (crystal-like lattices): stacks of crystalline lamellae in semicrystalline polymers or ordered microphases in form of lamellae, rods or spheres existing in block copolymers, etc. All these systems can be studied by means of scattering methods, providing that appropriate wavelength of radiation is choosen. Scattered intensity distribution in a case of such system can be written in form of Fourier transform of s.c. Q function[18] or Patterson function[25], being a special case of Q function for infinitely large crystal. The appropriate expression assumes form

$$I(\underset{\sim}{b}) = \int Q(\underset{\sim}{x}) \exp[-2\pi i(\underset{\sim}{b} \cdot \underset{\sim}{x})]dv_x \qquad (16)$$

where

$$Q(\underset{\sim}{x}) = \int \varrho(\underset{\sim}{y})\ \varrho(\underset{\sim}{x} + \underset{\sim}{y})dv_y \qquad (17)$$

is convolution square of the scattering power (electron density in the case of X-Ray scattering) and

$$|b| = \frac{2\sin\vartheta}{\lambda} \qquad (18)$$

The distribution of intensity scattered by ordered structures appears as a set of discrete maxima occuring at angular positions determined by Bragg law

$$n\ \lambda = 2d_{hkl}\ \sin\vartheta_{hkl} \qquad (19)$$

where d_{hkl} is interplanar distance for the planes having Miller indices (hkl), and ϑ_{hkl} is a glacing angle for intensity maximum corresponding to those planes. Equation (16) or its form simplified due to symmetry

$$I(hkl) = \Sigma\ Q(hkl)\ \cos[2\pi(hx + ku + lz)] \qquad (20)$$

can be used for studying the details of structure forming a three-dimensional lattice. Similar equations can also be written for linear and two-dimensional lattices[1,2,18].

The order in physically real objects is newer perfect. This lack of perfection, as well as finite size of ordered domains causes some effects in the scattered intensity distribution. These consist in broadening of individual lines, and also in changes of the intensities of individual lines as compared to those arising from ideal lattice. The effect of crystal size can be investigated by means of Scherrer equation

$$L_{hkl} = \frac{K \lambda}{\beta \cos\vartheta_{hkl}} \qquad (21)$$

where K is constant close to unity, β is true broadening of the diffraction line (after separation of instrumental broadening), and L_{hkl} is crystal size in the direction of reciprocal vector (hkl).

More recently Hosemann (cf.[18]) elaborated an approach basing on the concept of paracrystalline lattice allowing evaluation of not only average size of crystalline domains, but also the determination of distorsions occuring in the crystals. The effect of the distorsions of the first kind on the intensity of the diffraction line can be expressed in form[18,27,29]

$$D(m) = \exp(-4\pi^2 g_I^2 m^2) \qquad (22)$$

where $g_I = (\Delta d)_I/\bar{d}$ is the relative linear displacement, and m is the order of the reflection. Distorsions of the first kind occur in the case when long-range periodicity is preserved, and actual positions of scattering centers can be considered as resulting from small, statistical displacements from points of equilibrium, corresponding to ideal lattice points. In other words, the average position is identical as the ideal position of the scattering center in the lattice.

Distorsions of the second kind are connected with much bigger displacements, acting in such a way that average positions of structural elements do not correspond to any ideal lattice points. This kind of distorsions affects not only intensity but also causes broadening of the diffraction line. The effect on intensity is again expressed by means of exponential formula[27]

$$|F| = \exp(-2\pi^2 g_{II}^2 m^2) \qquad (23)$$

Broadening of the diffraction lines, can be written in turn as a sum of contributions from finite crystal size and from the distorsions. According to Hosemann at al.[27,28] the appropriate formula reads

$$(\delta s_o)^2 = \frac{1}{\bar{L}_{hkl}^2} + \frac{(\pi g_{II})^4 m^4}{d_{hkl}^2} \qquad (24)$$

An example of application of the eq.(24) is given in Fig.6.

A review of various methods of experimental determination of line broadening can be found in[26] and[29].

Dealing with polymeric materials one has to recognize that crystalline, ordered material usually coexist with amorphous one. Frequently it is of interest to establish proportions of these two components in a given sample of the material. Among great number of methods proposed in order to accomplish this task, one offered by Ruland[30], seems especially well justified from physical viewpoint. The degree of crystallinity is given[30] as

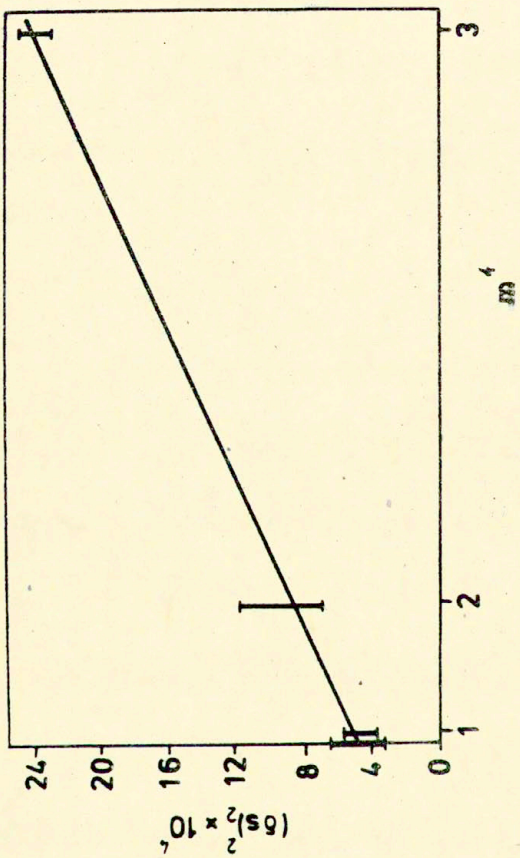

Fig. 6. Separation of the effects of crystal size and distorsions for hot-drawn polyethylene.

$$x_c = \frac{\int_0^\infty h^2 I_c(h)dh \quad \int_0^\infty h^2 \bar{f}^2(h)dh}{\int_0^\infty h^2 I(h)dh \quad \int_0^\infty h^2 \bar{f}^2(h)D\,dh} \qquad (25)$$

where $I_c(h)$ is crystalline contribution into total scattered intensity, $I(h)$, $\bar{f}(h)$ is average atomic scattering factor, and D is distorsion factor.

It can be seen from eq.(25) that the method compares experimentally measured intensities directly with atomic scattering factor, taking into account the effect of disorder. The approach requires absolute intensity measurements in wide range of scattering angles as well as application of a number of corrections. Since it is quite labor-consuming, the method is frequently replaced by simpler ones, basing on some kind of relative calibration (cf.[29]).

Another important example of ordered structure is linear lattice of lamellar crystals formed in semicrystalline polymers. Existence of such structure is manifested by occurence of maximum in small-angle region of X-Ray scattering. First attempt of quantitative analysis of this type of scattering was made by Tsvankin[19], basing upon simple model of electron density distribution. This model, later extended by Buchanan[32] can be used to determine the long period of the structure, c, as well as average thicknes of individual lamella, a. The ratio a/c provides information concerning linear crystallinity of the system.

A number of more complicated models, introducing distributions of lamellar sizes and interlamellar distances were proposed by Hosemann[18,20], Bramer and Wenig[33]. Correlation function approach, in turn, was offered by Vonk[11].

POSSIBLE STRUCTURES OF BINARY POLYMER BLENDS, AND METHODS OF THEIR CHARACTERIZATION

It is well known that frequently polymers do not mix at all or show only limited miscibility. The problem is usually known under the name of compatibility of polymers. This effect, together with usual partial crystallinity, and complex morphology of individual polymers, can produce a wide variety of possible structures in blend. Following part of the paper is dedicated to an attempt to classify possible structures and look for appropriate methods for their characterization. The classification of blended pairs is based upon the ability of each polymer to crystallize, and upon their mutual compatibility.

i. Both Components Amorphous

The simplest structural situation occurs when both polymers in the blend are not able to crystallize. In such a case compatible components are mixed on molecular level in similar way as long chain molecules dissolved in low molecular solvent. In the case of polymer blend chain molecules of one component are dispersed between similar chain molecules of polymer solvent. It is of interest to learn conformations of the molecules of each polymer in the blend, as well as to establish mutual interactions. Both factors mentioned, can be affected by temperature, concentration of the dissolved molecules in the matrix, etc. Analogy with the molecular solution in low molecular solvent brings in mind the possibility of similar methods of characterization. The neutron scattering performed on dilute blends of deuterium tagged macromolecules dissolved in normal (proton-containing) matrix prooved itself as very powerful technique for the case studied. According to[33] the relationship between scattered intensity, I, the magnitude of scattering vector, h, and molecular as well as thermodynamic characteristics of the system can be expressed in form

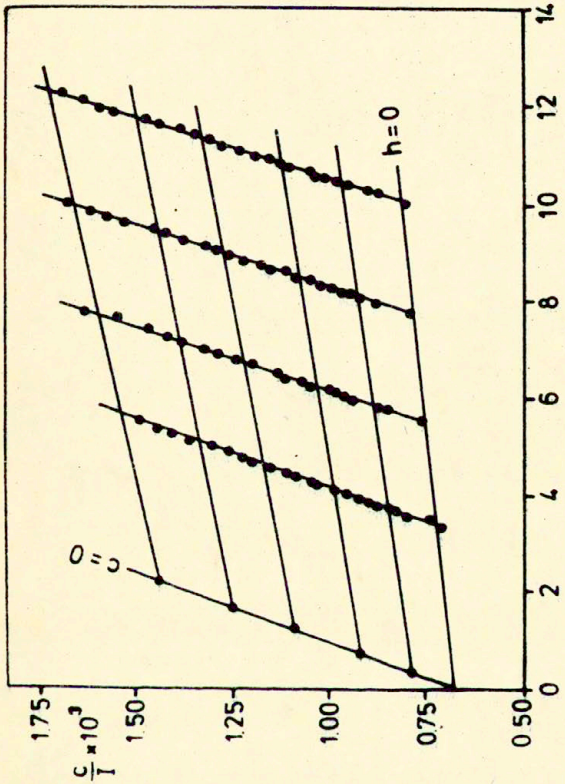

Fig. 7. Zimm-type plot for neutron scattering in dilute blend of deuterated polystyrene in the blend of poly(xylenol ether)

$$\frac{K^* c_2}{I} = \frac{1}{M_2}\left[1 + 4\gamma M_1 A_2 c_1\right] + \frac{h^2 \langle s \rangle_2^2}{3M_2} + 2A_2 c_2 \qquad (26)$$

where M_1, M_2, c_1, c_2 are molecular weights and concentrations of both components, respectively, $\gamma = \nu_2/\nu_1$ is the ratio of neutron contrast coefficients, $\langle s \rangle_2^2$ is mean square radius of gyration of component 2, and A_2 is second virial coefficient. The eq.(26) is analogous to that one describing light scattering from dilute polymer solutions, and can be used to construct classical Zimm plot in order to extrapolate experimental data to zero concentration and zero of scattering vector, h. An example of such plot is given in Fig.7, showing neutron scattering data[33] for blends of polystyrene and brominated poly(xylenol ether). Parameters evaluated by means of that plot are shown in Table 3 for three sets of blends differing in the degree of bromination of PBr_xXE. It is seen that small changes of molecular size parameter $\langle s^2 \rangle_2^{\frac{1}{2}}$ are accompanied with quite large differences in second viril coefficient and interaction parameter when the bromine content, x, increases above 0.4 . The values of interaction parameter show that in the third blend (cf. Table 3) some incompatibility occurs, while first two mixtures appear to be compatible.

Another possible source of information concerning this class of blends can be wide-angle neutron or X-Ray scattering analysed through the radial distribution function. It would give an information about local order. The information could possibly be evaluated by comparison of RDF's for pure components and their blends. No example of this kind of analysis can be given so far. An example of slightly different approach is given in[35] for blends of polycaprolactone and poly(vinyl chloride) (PCL/PVC). Basing on microscopy and DSC measurements, it was concluded that blends having high concentration of PVC are amorphous and behave as compatible. X-Ray scattering at small angles was interpreted in terms of correlation function

Table 3

Molecular and thermodynamic parameters for 50/50 blends of polystyrene and brominated poly(xylenol ether) obtained by means of neutron scattering[33] on small addition od deuterated polystyrene

BROMINE CONTENT atoms/monomer	$\langle h^2 \rangle^{\frac{1}{2}}$	$A_2 \cdot 10^4$	χ_{20}
0	35.8	0.44	-0.0044
0.4	36.5	0.31	-0.0029
0.084	34.5	0.075	+0.0005

(cf.eq.10) under assumption of random dispersion of components. In this case[6,9] correlation function assumes exponential form

$$\gamma(r) = \exp(-r/a) \tag{27}$$

where, a, is the correlation distance. Integration of eq.(11) with this form of correlation function gives the following expression for the intensity

$$[I(h)]^{-\frac{1}{2}} = \frac{K}{(a^3 \bar{\eta}^2)^{\frac{1}{2}}} (1 + h^2 a^2) \tag{28}$$

If the eq.(28) holds, the plot of $(I)^{-\frac{1}{2}}$ vs. h^2 should lead to a straight line, from which, a^2, and $\bar{\eta}^2$, could be evaluated. This kind of plot is shown in Fig.8, where, $I^{-\frac{1}{2}}$ is plotted vs. Θ^2, giving rather food approximation for small angles. As it is seen, straight lines are indeed obtained. According to Kratky[36], the correlation distance, a, is related to an average chord length

$$\ell_i = a/\varphi_i \tag{29}$$

where, φ_i is the volume fraction of phase i. The idea of average chord length, or average inhomogeneity length, is explained in Fig.9. It represents an average length of parts passing through the same phase, and belonging to chords crossing the material in various directions. For the case of two-phase medium, the average chord length satisfy the relationship

$$\frac{1}{\ell_c} = \frac{1}{\ell_1} + \frac{1}{\ell_2} \tag{30}$$

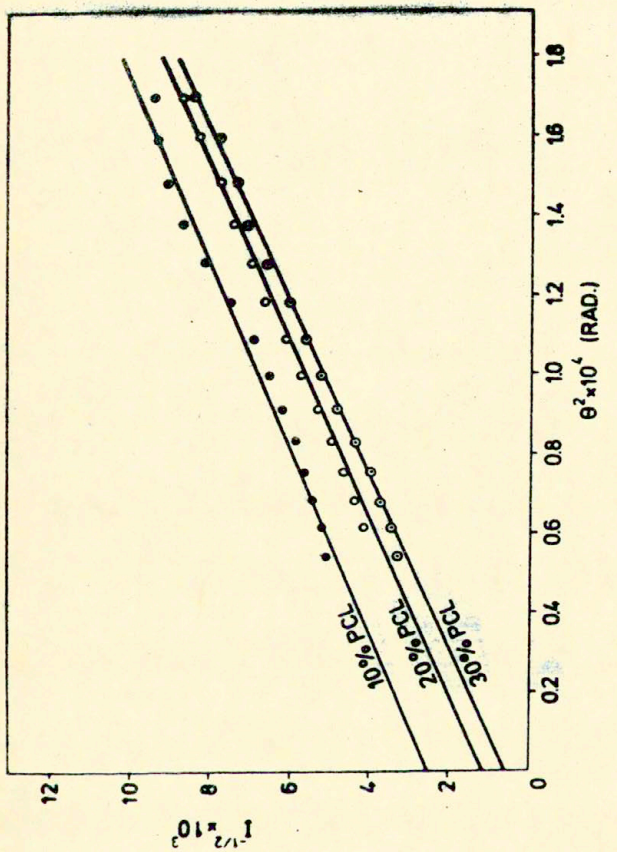

Fig. 8. Application of angular relationship for intensity, derived from exponential correlation function, to interpretation of SAXS data from PCL/PVC blend.

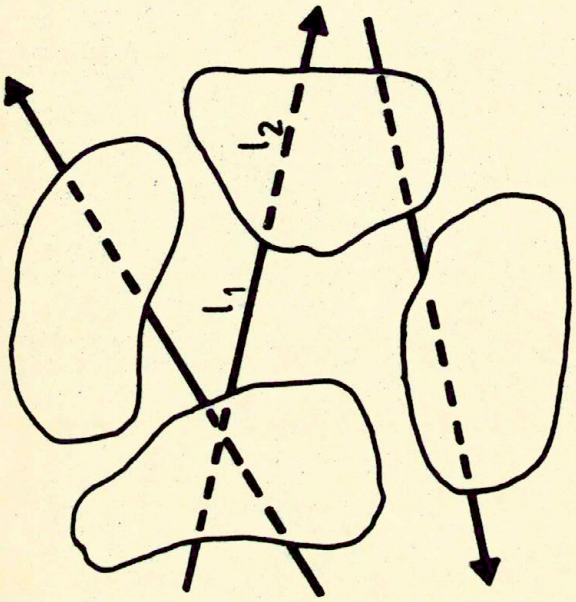

Fig. 9. Illustration of the idea of average chord length.

Results obtained[35] for PCL/PVC blends are shown in Fig.10. It is clearly visible that at low PCL concentrations, l_{PCL}, is small and comparable with molecular dimensions of single molecule. An increase of PCL concentration causes an increase of, l_{PCL}, to the values indicating aggregation of molecules, and occurence of bigger domains of PCL. Consequently, it can be interpreted as an increase of incompatibility of the system with the increase of PCL concentration.

The method described above offers, therefore, also a possibility to investigate amorphous blends in which components are incompatible. It has to be noted, that the method is sensitive enough to detect presence of domains slightly etending the molecular dimensions of single polymeric molecule.

A possibility for analysis of amorphous blends of incompatible components, being a dilute system of domains of one polymer randomly distributed in a matrix formed by the other, is offerred by Guinier's law. The intensity of radiation scattered by such a system in a range of very small angles is given by an approximate formula

$$I(h) = I(0) \exp(-\tfrac{1}{3} h^2 R_g^2 + \ldots) \qquad (31)$$

Plotting $\ln[I(h)]$ vs. h^2 (cf. Fig.11) yields straight line plot, enabling direct determination of the average radius of gyration, R_g, of the domain.

When the domains appear to be more densely packed eq.(28) can be still applicable, whereas Guinier law (eq.31) is no more valid.

Some of structural parameters can be defined through integrals of scattered intensity. Porod[37,38] have defined a scattering invariant as

$$Q = 4\pi \int_0^\infty h^2 I(h) dh \qquad (32)$$

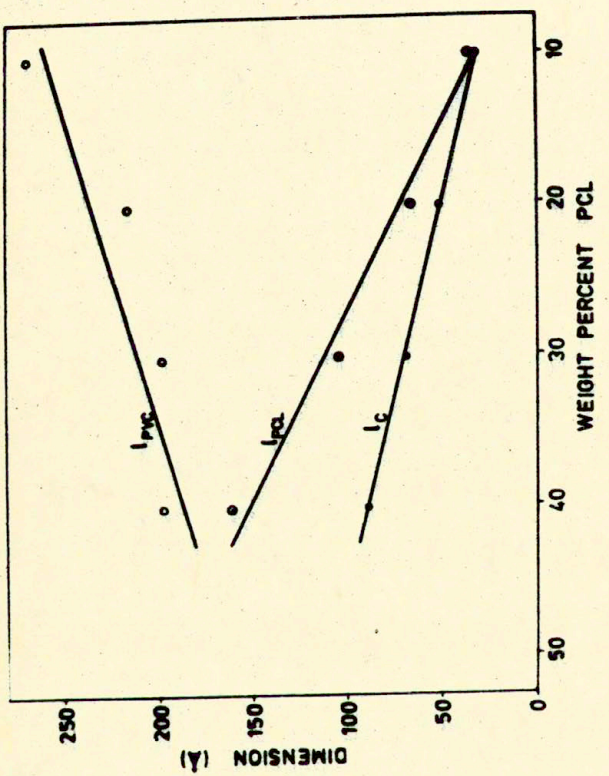

Fig. 10. Average chord lengths for PVC and PCL as a function of blend composition.

and shown that it is related to scattering power of the system, $\bar{\eta}^2$. In a case of two-phase system the scattering power can be expressed as

$$\bar{\eta}^2 = \varphi_1\varphi_2(\varrho_1 - \varrho_2)^2 \qquad (33)$$

where φ_1, φ_2 are volume fractions and ϱ_1, ϱ_2 are electron densities of the coexisting phases.

A correlation length, l_c, the other parameter characterizing dimensions of inhomogeneities is defined as follows

$$l_c = 2\int_0^\infty \gamma(r)dr = \frac{2\pi\int_0^\infty h\, I(h)dh}{Q} \qquad (34)$$

Characteristic dimensions of inhomogeneities (domains) can be also evaluated from the behavior of the SAXS curve at relatively large angles. The following relationship, known as Porod's law[37,38] reads

$$\lim_{h\to\infty} I(h) = \frac{K_p}{h^4} \qquad (35)$$

where K_p is Porod's constant, which in turn is related to the area of the interface per unit volume (S/V)

$$K_p = \frac{(S/V)Q}{8\pi^3\,\varphi_1\varphi_2} \qquad (36a)$$

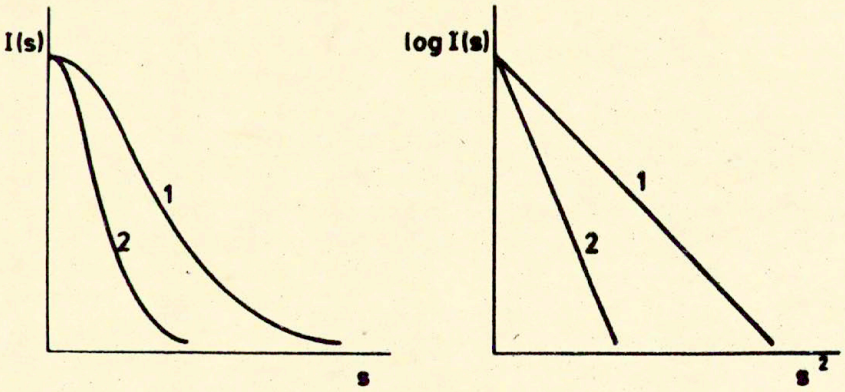

Fig. 11. SAXS intensity distribution from a system of independent scatterers.
a. Intensity as a function of scattering vector,
b. Guinier's plot.

and to inhomogeneity length, l_p

$$K_p = \frac{Q}{2\pi^3 l_p} \tag{36b}$$

Porod's law in form of equation (35) holds only in cases when coexisting phases are separated with sharp boundaries. Usually, the interface boundaries are not sharp, but showing some diffuse profile. Determination of the shape and extent of this profile is of great interest in the blend characterization. Attempts made to elaborate the appropriate methods for this task[39-42] are reviewed in detail with examples of application in[42]. The idea, common for all the treatments is ilustrated in Fig.12. It consist in convoluting a function describing the ideal sharp boundary with some kind of smoothing function. Electron density profile, constructed that way, is then used to derive a modified version of Porod's law. As an example, the formula obtained[39] for the case of gaussian smoothing function can be given

$$I(h) = \frac{K_p}{s^4} \exp(-4\pi^2\sigma^2h^2) \tag{37}$$

where σ is a half-width of smoothing function (cf. Fig.12). The parameter, σ, can be evaluated experimentally by means of appropriate plot basing on eq.(37).

Another effect connected with diffuse boundaries, as indicated in[35], is a reduction of scattering power $\bar{\eta}^2$. Basing on the assumption of linear gradient of density, the following expression was proposed

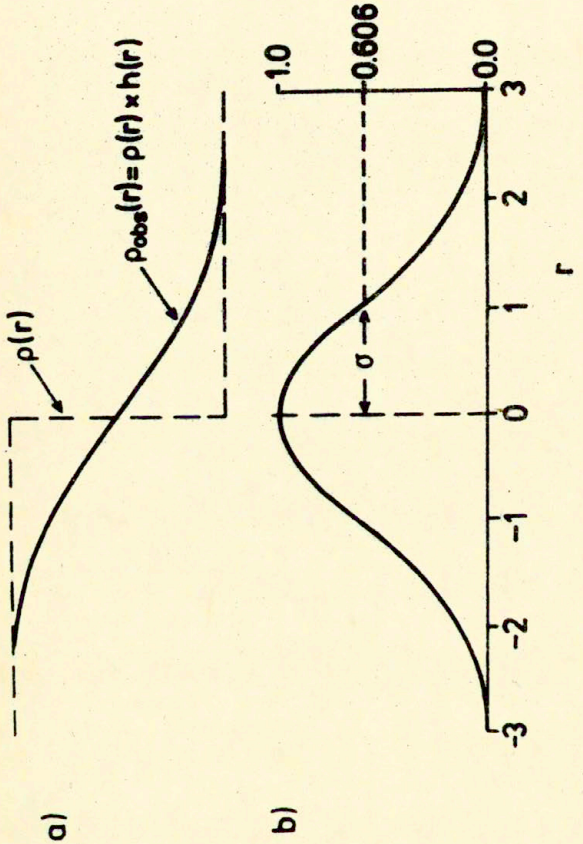

Fig. 12. Density profile at the interface
a. sharp and diffuse boundaries
b. smoothing function

$$\bar{\eta}^2 = (\varrho_1 - \varrho_2)^2(\varphi_1\varphi_2 - \varphi_3/6) \qquad (38)$$

where φ_3 is volume fraction of the interface zone.

ii. One Component Partly Crystalline

More complicated situation occurs when one of the components of the blend is crystallizable. In such a case various morphologies might exist depending upon eventual compatibility of components in amorphous phase. As a simples case one can imagine two-phase morphology formed from separate crystals of one component embedded into uniform, amorphous matrix containing both components in some concentrations. The concentration of components in amorphous phase would depend on composition of the blend, and on its crystallinity. This kind of a system with random distribution of crystals would give Guinier type of X-Ray scattering (cf.eq.31) at small angles. In such a case the size of crystals could be estimated from eq.(31), basing on the slope of the intensity function. It seems also possible, that slope of Guiner's plot will change with an increase of scattering angle, indicating also some details of molecular dimensions of components in the amorphous phase. The other source of data indicating dimensions of crystals can be measurement of integral characteristics of scattered intensity, and application of eq.(34).

The existence of diffuse boundary between the crystal and amorphous phase can be pressumed in the mixed systems containing one crystallizable component. It is also possible that the diffuse boundary in this case would have more complicated structure than in pure crystalline polymer, since concentration gradient might occur in the vicinity of the crystal even in the case of completely miscible amorphous surrounding. The profile of density distribution in the diffuse boundary still should be accessible through analysis of the deviations from Porod's law (cf. eq.37).

Simultaneously WAXD measurements can be used to determine the degree of crystallinity, defined as ratio of the volume of crystalline phase to the total volume of the system. The method of determination might make use of eq.(24). Size of the crystals, and distorsions of their periodicity both affect the WAXD lines and can be estimated basing on the equations (20-23).

Depending upon the size of crystals and on their anisotropy, some light scattering might also occur in such a system. The scattering pattern would extend to rather broad range of angles, and reveal geometrical and optical properties of the crystal as well as polarizability difference between the crystal and surrounding matrix.

A little more complicated case may occur when the components of the blend are not compatible in amorphous phase. In this case crystals are not single reason for inhomogeneity of the system. Also domains of one amorphous component distributed in the matrix formed by second one, contribute to inhomogeneity, and consequently also contribute to the scattering. Especially SAXS can be affected, however, it is not simple to distinguish between contributions of both: crystalline and amorphous domains. Probably, analysing distributions of inhomogeneity lengths, as well as performing some model considerations concerning the scattering power of the system, one could get insight into this problem.

The existence of amorphous domains, due to incompatibility of amorphous phase, in turn, should not substantially affect the WAXD pattern. In some fortunate cases the shape of amorphous halo could change, giving evidence of amorphous phase separation. In majority of cases, however, this effect will not be too easy to recognize. The determination of the degree of crystallinity based on separation of crystalline peaks should not bring much more difficulties, than one encounters in the case of amorphous phase built of compatible components.

The existence of amorphous domains can also give rise to an increase of turbidity of the system, and contribute to V_V mode of light scattering.

Crystals in these systems, instead of being randomly

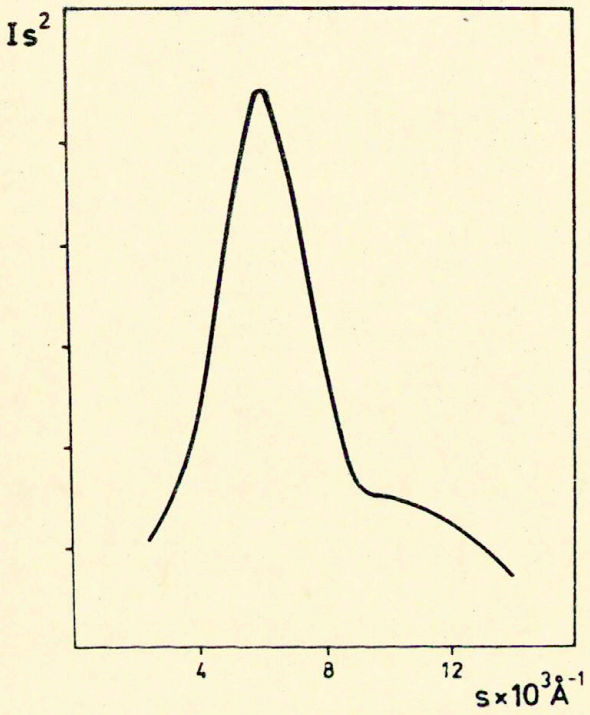

Fig. 13. SAXS intensity distribution for a stack of lamellar crystals.

distributed, might form ordered linear macrolattices ar macroparacrystals distributed in amorphous matrix. Such a case would evidently manifest itself in SAXS, giving clear maximum at some scattering angle. An example of such a pattern is given in Fig.13. Analysis of this kind of intensity distribution is usually performed basing on model consideration[18-20, 32,33] or using the idea of correlation function[11]. In the simplest models[19,32] a stack of the lamellae with trapezoidal electron density profile is discussed (cf. Fig.14). Long period, c, of the structure is defined as a sum of lamellar thickness, a, and interlamellar distance, l

$$c = a + l \tag{39}$$

Linear crystallinity, k, is then

$$k = \frac{a}{c} \tag{40}$$

Basing on Fourier transform of electron density distribution, calibration plots are computed and can be used for determination of the model parameters from the experimental intensity curve. More sophisticated models, e.g.[20,32,33] assume occurence of distributions of lamellar sizes and interlamellar distance as well as some correlations (to avoid an effect of overlapping of the lamellae). The are usually used by means of direct fitting of model-calculated intensity distribution to the measured one.

Calculation of the correlation function[11] directly by means of Fourier transform of scattered intensity distribution is also a possible route for structure evaluation. Computation of the correlation function is then followed by fitting to some model calculated one. This kind of procedure was recently applied to iPS/aPS and /CL/PVC blends[43,44].

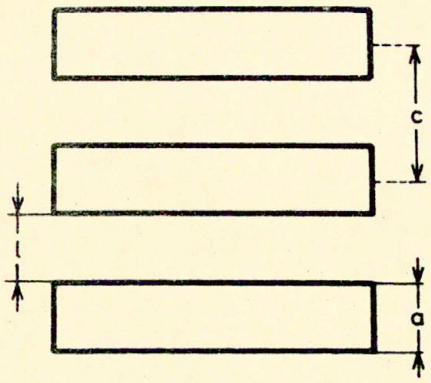

a.

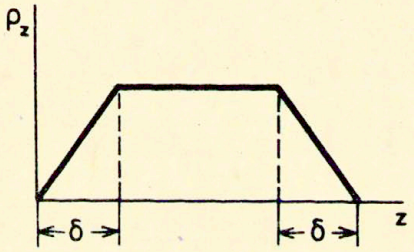

b.

Fig. 14. a) The model of a stack of lamellar crystals
b) Trapezoidal intensity profile

An example[44] of such correlation fucntion is shown in Fig.15.

Usually, stacks of crystalline lamellae are arranged into higher-order morphology forming e.g. well-known spherulites. Again, the structure might reveal a variety of cases. The simplest case occur when sperulites, containing crystals of one component, are embedded in the amorphous, mixed matrix. Even in this case a question might rise whether or not the amorphous part contained within the spherulite has the same composition as the matrix outside. The answer to this question is very important one, when crystallization mechanisms are concerned.

Analysis of the spherulite sizes as well as more sophisticated problems concerning details of the internal structure of the spherulite (tangential and radial polarizabilities) might be determined from SALS measurements in H_V mode. Very simple data are needed for spherulite size determination, whereas more precise, and absolute values of scattered intensities are required for polarizability evaluation. Adding absolute SALS measurements in $V_V$mode, one can also obtain an average polarizability of the matrix surrounding the spherulite and the degree of volume filling (cf. eq.13a, 13b).

Similar system, in which components in amorphous phase are incompatible, reveal some new structural possibilities. Separate spherulities of crystallizable component embedded in uniform matrix of the other one, as well as in the matrix containing amorphous domains of the first component, can be considered as one of the variants. Sperulites containing crystalline lamellae of one component, together with amorphous domains of both components, again embedded into domain-structured amorphous matrix containing also both components is the second variant. Actual theories of SALS provide tools for analysis of scattering data, sufficient to determine the spherulite structure of first case. Theoretical tool, however, sufficient for direct interpretation of light scattering from structures, in which amorphous domains coexist, or even are built into spherulites, does not exist so far. In such cases, however, some conclusions might be drawn basing partly on

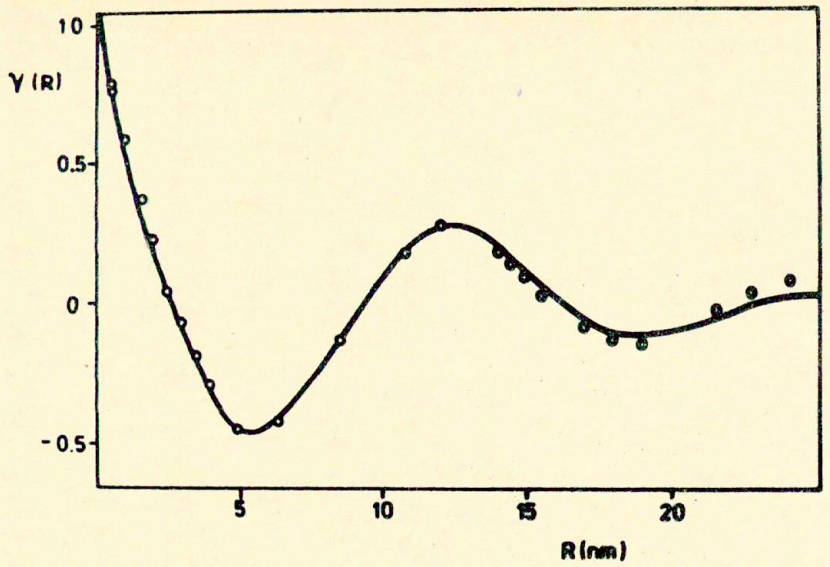

Fig. 15. Correlation function describing lamellar structure of PCL/PVC semi-crystalline blend. Solid line - model calculated, points - computed from experimental data.

classical theories of light scattering, and partly on additional information obtained by means of other methods (e.g. microscopy, calorimetry etc.).

iii. Both Components Partly Crystalline

Blends made of both crystallizable components might form more complicated structures than any one of groups already discussed. The new possibilities consist in simultaneous existence of crystals of both components embedded into uniform (in case of compatibility) or heterogeneous amorphous matrix. The degree of crystallinity, total and/or separate for each component (usually refered to total volume of amorphous phase) can be determined in usual way from WAXD. A possibility of co-crystallization become another problem of interest, which also can be studied in frame of WAXD results. One can expect two modes of co-crystallization. The first consist in replacements of molecules of one component by molecules of the other, preserving the crystallographic lattice of the first component. This kind of replacements would only be accompanied by relatively small change in lattice constants. Consequently WAXD diagram would consist of the same lines as one obtained from crystals of pure component, showing only some shift in their positions. Since the structure factors of crystallographic planes would be affected accordingly to the scattering power of "foreign" molecules as well as to the character of order in replacements, the intensities of the diffraction lines might also depend upon the blend composition. Character of the dependences of lattice constants and line intensities upon the blend composition, therefore might be affected by nuances of the structure of mixed crystal. In a case of limited miscibility in crystalline state, the coexistence of two structures: the solution of first component in the second one, and the solution of the second component in the first, could be expected. This case would manifest itself in overlapping of X-Ray diagrams corresponding to crystal lattices of both solid solutions. The other possibility consist in formation of the completely new crystal structure. The crystal of the blend

would then be characterized by a set of diffraction lines different than those corresponding toeach pure component. This kind of mixed crystallization would be probably the easiest to detect.

It is usual opinion that mixed crystallization cannot be frequently expected in polymeric systems. In fact only one case was so far reported[45]. This was a set of blends of polypropylene with polybutene-1, crystallized under high elongational gradients. Basing on preliminary X-Ray investigation[45] and some other measurements the possibility of mixed crystallization was suggested. Further investigations[46,47] performed on the same samples indicate the presence of two crystalline phases. Crystal size and amount of the disorder of each phase appear to be dependent upon sample composition, whereas small shifts of line positions (from those, corresponding to pure components crystallized under quiescent conditions) are found independent of blend composition. These results evidently exclude the possibility of occurence of mixed crystals having crystal structure different than structures of pure components. The results, however, do not offer enough arguments neither to support nor to reject the hypothesis concerning existence of solid solution type of mixed crystals with small concentration of the solute and random mixing of molecules in the crystal lattice (random replacements, that would not affect relative intensities of diffraction lines).

Morphological features in the particular case of PP/PB-1 crystallized from oriented melt[45] are quite exeptional. Occurence of needle-like crystals was demonstrated by electron microscopy[45]. Lateral sizes of these crystals determined[46] by means of SAXS using Guiner-type of analysis appear to be nearly independent of blend composition. Due to apparent contradiction to WAXD results it was concluded that real dependencies are obscured by compensation effects connected to opposite behaviors of crystal sizes of both components.

In more usual cases involving isotropic crystallization, a spherulitic morphology can be expected. The detail of this morphology to some extend can be studied by means of SAXS and SALS. Various problems, however, might be encountered during

intepretation of results. Using theoretical tools already existing, only average parameters, characterizing all existing phases can be determined. Development of model calculations, dedicated to particular systems might bring some progress. Combining scattering techniques with other methods might also bring valuable informations and help in understanding of complicated structures.

The difficulties become more enhanced, in most frequent cases, when the system does not form any mixed crystals. In this case, even with components compatible in amorphous phase, complicated morphologies must form due to coexistence of separate crystals of both components. The problems concerning the structure of superstructural aggregates like bi-component lamellar stacks or spherulites, are still unsolved. Experiments reported in[48] for PET/PBT blends in some range of compositions indicate the existence of separate spherulites formed by both components at low degrees of supercooling. Less perfect, mixed spherulites, containing separate crystals of both components were found at higher concentration of the second component. Further increase of this concentration yields in non-spherulitic morphology. Light scattering examination shows that character of H_V pattern changes from $0-90^\circ$ type, observed in pure PBT to 45° type in a blend containing small (10%) concentration of PET. It is concluded that the presence of the other polymer (PET) affects the growth habit of PBT crystals in a manner sufficient to change optical properties of the spherulite. This example indicates that at least in some fortunate cases relatively deep conclusions might be drawn from simple measurements even performed in such complicated systems. It ha has to be noted, however, that more detailed, quantitative description of the structure would produce quite severe problems so far.

iv. Oriented Systems

In many situations, when polymeric material is formed under stress (e.g. fiber spinning, drawing extrusion) anisotropic, oriented textures appear in addition to eventual

deformation of structural elements.

Quantitatively, the texture (preferred orientation) can be described by means of orientation distribution function.

$$w(\xi,\varphi,\eta) = \frac{dN}{N}\Bigg|_{\substack{\xi,\xi+d\xi \\ \varphi,\varphi+d\varphi \\ \eta,\eta+d\eta}} \tag{41}$$

where $\xi = \cos\vartheta$, and ϑ,φ,η are Euler angles. It gives the fraction dN/N of structural elements having their axes in particular range of Euler angles, and N is total number of elements having their axes in particular range of Euler angles (dN is a number of elements in the infinizitemal range of Euler angles and N is total number of elements in the system). Function $w(\xi,\varphi,\eta)$ fulfilles the normalization condition

$$\int_0^{2\pi}\int_0^{2\pi}\int_{-1}^{1} w(\xi,\varphi,\eta)\,d\xi\,d\varphi\,d\eta = 1 \tag{42}$$

The orientation distribution $w(\xi,\varphi,\eta)$ cannot be measured directly. For the case of crystals being structural elements, another function can be define, giving the orientation distribution for j-th reciprocal vector. This function can be directly measured from WAXD azimuthal intensity profile. According to early analysis by Roe and Krigbaum[49], followed by extended approaches[50-52], there exist a relationship between these functions. This relation can be obtained[51] by expanding both functions into a series of normalized, generalized spherical harmonics

$$\omega(\xi,\varphi,\eta) = \sum_{l=0}^{\infty} \sum_{m=-l}^{l} \sum_{n=-l}^{l} W_{lmn} Z_{lmn}(\xi) \exp\{-i(m\varphi + n\eta)\} \qquad (43)$$

and

$$q^j(\zeta_j,\varphi_j) = \sum_{l=0}^{\infty} \sum_{m=-l}^{l} Q_{lm}^j \Pi_l^m(\zeta_j) \exp(-im\varphi_j) \qquad (44)$$

where coefficients W_{lmn} and Q_{lm}^j are given by

$$W_{lmn} = \frac{1}{4\pi^2} \int_0^{2\pi} \int_0^{2\pi} \int_{-1}^{1} \omega(\xi,\varphi,\eta) Z_{lmn}(\xi) \exp\{i(m\varphi + n\eta)\} d\xi d\varphi d\eta \qquad (45)$$

and

$$Q_{lm}^j = \frac{1}{2\pi} \int_0^{2\pi} \int_{-1}^{1} q^j(\zeta_j,\varphi_j) \Pi_l^m(\zeta_j) \exp(im\varphi_j) d\zeta_j d\varphi_j \qquad (46)$$

The functions $Z_{lmn}(x)$ and $\Pi_l^m(x)$ are

$$Z_{lmn}(x) = \left[\frac{2l+1}{2} \frac{(l-m)!}{(l-n)!} \frac{(l+m)!}{(l+n)!}\right]^{\frac{1}{2}} \times$$

$$\times \frac{1}{2^m}(1-x)^{2(m-n)}(1+x)^{\frac{m+n}{2}} P_{l-m}^{(m-n,m+n)}(x) \qquad (47)$$

where $P_{l-m}^{(m-n,m+n)}(x)$ is Jacobi polynomial, and

$$\Pi_l^m(x) = \left[\frac{2l+1}{2}\,\frac{(l-m)!}{(l+m)!}\right]^{\frac{1}{2}} P_l^m(x) \qquad (48)$$

where $P_l^m(x)$ is asseciated Legendre polynomial.

After application of an addition theorem for spherical functions, and some other operations the following equation is obtained

$$Q_{lm}^j = 2\pi\left(\frac{2}{2l+1}\right)^{\frac{1}{2}} \sum_{n=-l}^{l} W_{lmn}(\cos\Theta_j)\exp(in\Phi_j) \qquad (49)$$

where Θ_j and Φ_j are angular coordinates of j-th reciprocal vector fixed within the crystal.

It is seen therefore that equation (49) gives a relationship between coefficients Q_{lm}^j of expansion of experimentally measured function $q^j(\zeta_j,\varphi_j)$ and coefficients W_{lmn}, determining the unknown function $w(\xi,\varphi,\eta)$. Depending upon required accuracy of approximation (a number of expansion terms), the coefficients Q_{lm}^j should be obtained for approriate number of reciprocal vectors. Then, coefficients W_{lmn} can be computed by solving the set of linear equations based on eq.(49). In some cases, when particular symmetry of texture is observed equations (43 - 49) can be reduced to simpler forms. Nevertheless, in any case determination of the coefficients W_{lmn}, in order to approximate the orientation distribution function $w(\xi,\varphi,\eta)$ with reasonable accuracy, requires aquisition of quite substantial amount of experimental data, as well as labor consuming computations. Therefore, in many practical cases, this procedure is replaced by simpler means of description of orientation (cf.[29]). The most popular makes use of the moments of experimentally measured $q^j(\zeta_j,\varphi_j)$ orientation distribution, without further computations. In cases of uniaxial symmetry (the distribution independent of φ_j), the procedure is usually

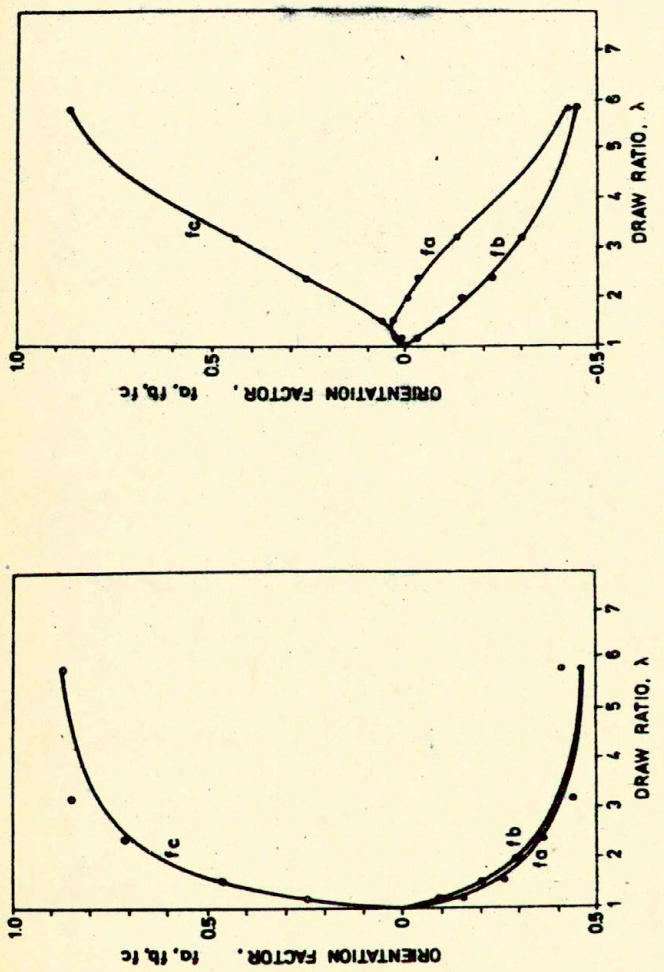

Fig. 16. Crystal orientation factors for polyethylene (a) and polypropylene (b) in 50/50 PE/PP blend as functions of draw ratio.

limited to determination of only second term of expansion, what yields in s.c. orientation factor

$$f = \frac{3\langle\cos^2\vartheta\rangle - 1}{2} \qquad (50)$$

This orientation factor is used to describe the orientation distribution of particular reciprocal vectors or crystallographic axes, as well as to follow their dependencies upon external factors.

Even this simplified approach, quite frequently applied to various problems of polymer physics, is rather rare in studies of polymer blends. Pioniering work by Oda, Maeda and Hibi[53] concern an examination of dependencies of orientation factor upon deformation of PE/PP blend for three main crystallographic axes of crystals of both components. Results of these studies are shown in Fig.16a and 16b. Similar work was recently done by Min at al.[54], where orientation of PE crystals was studied in a melt spinning process of PE/PS blends. It is demonstrated, that blending strongly affects orientation of PE crystals even at conditions when spinning stress is maintained constant.

CONCLUDING REMARKS

The aim of this paper was to demonstrate that a variety of structures and morphologies that might occur in polymer blends can be studied by means of a number of methods involving scattering of diverse kinds of radiations. Application of different radiations enables to obtain informations about various levels of structure as well as to distinguish between scattering bodies of similar size but different physical constitution. A short summary of structures that might exist in blended polymeric systems is given in Table 4 with indication of problems that may be of interest for studies. An appropriate

Table 4

Possible structures in polymeric blends

A	B	(A + B) structures and problems
1 amorphous	amorphous	i) compatible size and conformation of molecules of both components as functions of concentration, conditions of formation and chemical composition of the blend. ii) incompatible degree of dispersion, size and shape of domains of one phase in the other, structure of the diffuse-boundary between phases.
2 amorphous	crystalline	i) amorphous phases compatible lamellar crystals of spherulites of B uniformly dispersed in amorphous matrix (A+B), volume filling system or dispersed spherulites containing lamellar crystals of B and mixed amorphous phase surrounded by mixed amorphous phase (A+B). crystallinity crystal structure of B morphology structure of spherulite structure of the diffuse boundary between phases. ii) amorphous phases incompatible lamellar crystals of B dispersed in inhomogeneous amorphous matrix composed of domains of A and B, partly crystalline spherulites of pure B dispersed in amorphous matrix of A, volume filling system with spherulites composed of lamellar crystals of B mixed with amorphous domains of A and B,

		mixed spherulites as above dispersed in a matrix of pure amorphous A or inhomogeneous one composed of domains of A and B. as in i), and degree of dispersion for each amorphous component.
3 crystalline crystalline	i) amorphous phases compatible	mixture of separate lamellar crystals of A and B dispersed in mixed materix (A+B), mixed crystals (A+B), due to co-crystallization, dispersed in mixed matrix, separate spherulites of A and B dispersed in mixed matrix, spherulites composed of mixture of crystals of A and B dispersed in mixed matrix, volume filling system of separate spherulites of each component, volume filling system of spherulites containing both components.
	ii) amorphous phases incompatible	separate crystals and separate amorphous domains mixed together, separate spherulites of each component (volume filling or dispersed in inhomogeneous matrix), spherulites containing crystals of both components (separate or mixed) and amorphous domains of one or both components (volume filling or dispersed in inhomogeneous amorphous phase). degree of crystallinity crystal structure or structures morphology structure of spherulites degree of dispersion diffuse-boundaries between various phases.

Table 5

Scattering techniques and applications

radiation	A^o	technique	applications
X-Rays	0.5 - 2.5	WAXD $0.1<h<25$ (A^{o-1})	atomic arrangements (distances) in liquid and amorphous solid (1 - 20 A^o) structure of crystal lattices defects in crystals crystallinity, orientation of crystals.
		SAXS $0.005<h<0.15$ (A^{o-1})	correlations of fluctuations in density of amorphous solids, degree of dispersion, conformation and dimensions, of individual chain molecule in dilute solution, structure of the stack of lamellar crystals in semicrystalline polymers, density distribution in the diffuse-boundary between phases, "linear" crystallinity.
electrons	comparable with WAXD		
neutrons	1.2	WANS $0.1<h<5$ (A^{o-1})	as in WAXD, and magnetic structures.

	1 - 15	SANS $0.01<h<0.15$ (A^{o-1})	as in SAXS, and conformation of deuterium tagged molecules in amorphous hydrogenated matrix, conformation of tagged macromolecules in crystalline polymer, compatibility.
light	4000-6000	WALS $3\cdot10^{-4}<h<2\cdot10^{-3}$ (A^{o-1})	studies on macromolecules in dilute solutions
		SALS $1.5\cdot10^{-5}<h<1.5\cdot10^{-3}$ (A^{o-1})	size and shape (deformation truncation) of spherulites, tangential and radial polarizability difference in spherulite, matrix polarizability, degree of volume filling.
microwaves	10^{7} - 10^{8}		characterization of composites (reinforced with short cut fibers or small spheres), characterization of blends with large domains.

choise of the character of radiation opens a number of possibilities for characterization of these complicated structures, and quite often for studies of interactions responsible for occurence and stability of the structures. A comparison of some physical features of various radiations as well as examples of possible applications are presented in Table 5.

REFERENCES

1. A.Guinier, G.Fournet, Small angle scattering of X-Rays, N.Y. 1955
2. A.Guinier, Théorie et Technique de la Radiocristallographie, Paris 1956
3. G.Porod, Acta Physica Austriaca, 2, 255, (1948)
4. R.S.Stein, M.B.Rhodes, J.Appl.Phys., 31, 1873, (1960)
5. R.S.Stein. in "Structure and Properties of Polymer Films" ed. by R.W.Lenz and R.S.Stein, Plenum N.Y. 1973, p.1.
6. P.Debye, J.Appl.Phys., 15, 338, (1944)
7. P.Mittelbach, G.Porod, Acta Phys.Austriaca, 14, 185, 405, (1961); ibid. 15, 122, (1962)
8. P.Mittelbach, Acta Phys.Austriaca, 19, 53, (1965)
9. P.Debye, A.Bueche, J.Appl.Phys., 20, 518, (1949)
10. P.Debye, H.R.Anderson Jr., H.Brumberger, J.Appl.Phys., 28, 679, (1957)
11. C.G.Vonk, G.Kortleve, Kolloid Z.,Z. Polym., 220, 19, (1967); 225, 124, (1968)
12. R.S.Stein, P.R.Wilson, J.Appl.Phys., 33, 1914, (1962)
13. P.Debye, J.Math.Phys., 4, 153, (1925)
14. S.M.Wecker, T.M.Davidson, J.B.Cohen, J.Mater.Sci., 7, 1249, (1972)
15. G.D.Wignall, G.W.Longman, J.Mater.Sci., 8, 1439, (1973)
16. E.W.Fischer, J.H.Wendorff, M.Dettenmaier, G.Lieser, Z.Voigt-Martin, Polymer Preprints, 15, no 2, 8, (1974)

17. M.R.Gupta, G.S.Y.Yeh, J.Macromol.Sci.-Phys., B15 (1), 119, (1978)

18. R.Hosemann, S.N.Bagchi, Direct analysis of Diffraction by Mater, North Holland Publ.Co, Amsterdam 1962

19. D.Ya.Tsvankin, Polymer Sci USSR, 6, 2304, 2310, (1969)

20. H.Beumer, R.Hosemann, J.Macromol.Sci.-Phys., B15 (1), 1, (1978)

21. R.S.Stein, M.B.Rhodes, J.Appl.Phys., 31, 1873, (1960)

22. R.J.Tabar, A.Wasiak, S.D.Hong, T.Yuasa, R.S.Stein, J.Polymer Sci., Pol.Phys. Ed., 16, , (1980)

23. D.Y.Yoon, R.S.Stein, J.Polymer Sci., Pol.Phys.Ed., 12, 763, (1974)

24. R.S.Stein, A.Misra, T.Yuasa, A.Wasiak, Polymer Preprints, 16 (1), 13, (1973)

25. M.J.Buerger, Vector space and its application to crystal--structure investigation, J.Wiley, N.York, 1959

26. A.Taylor, X-Ray Metallography, J.Wiley, N.Y., 1961

27. R.Bonart, R.Hosemann, R.L.McCullough Polymer, 4, 199, (1963)

28. R.Hosemann, W.Wilke, Faserforsch Textiltechnik, 15, 521, (1964)

29. L.E.Alexander, X-Ray Diffraction Methods in Polymer Science, Wiley-Interscience, N.Y. 1969

30. W.Ruland, Acta Cryst., 14, 1180, (1961)

31. D.R.Buchanan, J.Polym.Sci., A2, 9, 645, (1971)

32. W.Wenig, R.Brämer, Colloid Polym.Sci., 256, 125, (1978)

33. A.Maconnachie, R.P.Kambour, R.C.Bopp, 27th International Symposium on Macromolecules, p.1227, Strassbourg 1981

34. J.Jelenic, R.G.Kirste, B.J.Schmitt, S.Schmitt-Strecker, Makro-Mainz Preprints, p.908, (1979)

35. F.B.Khambatta, F.Warner, T.Russel, R.S.Stein, J.Polym.Sci., 14, 1391, (1976)

36. O.Kratky, Pure Appl.Chem., 12, 483, (1966)

37. G.Porod, Kolloid Z., 124, 83, (1951)

38. G.Porod, Kolloid Z., 133, 51, (1953)

39. W.Ruland, J.Appl.Cryst., 4, 70, (1971)

40. C.G.Vonk, J.Appl.Cryst., 6, 81, (1973)

41. T.Hashimoto, H.Kawai, Macromolecules, 10 (2), 377, (1977)

42. J.T.Koberstein, B.Morra, R.S.Stein, J.Appl.Cryst., 13, 34, (1980)

43. F.P.Warner, W.J.MacKnight, R.S.Stein, J.Polym.Sci.Phys., 15, 2113, (1977)

44. T.P.Russel, F.P.Warner, R.S.Stein, Makro-Mainz Preprints, p.924, (1979)

45. R.M.Gohil, J.Peterman, J.Macromol.Sci.Phys. Ed., B18, 217, (1980)

46. A.Wasiak, W.Wenig, J.Polym.Sci. (in preparation)

47. A.Wasiak, W.Wenig, (to be published)

48. R.S.Stein, F.H.Khambatta, F.P.Warner, T.Russel, A.Escala, E.Balizer, J.Pol.Sci..

49. R.J.Roe, W.R.Krigbaum, J.Chem.Phys., 40, 2608, (1964)

50. H.J.Bunge, Mathematische Methoden der Texturanalyse, Akademie Verlag, Berlin 1969

51. S.Nomura, H.Kawai, I.Kimura, M.Kagiyama, J.Polym.Sci., A2, 8, 383, (1970)

52. H.Kawai (edit.), Polymer Orientation, Spherulite Deformation and Anisotropy of Semicrystalline Polymers in Bulk, vol.I and II, Dept. of Polymer Chem., Kyoto Univ. 1979

53. A.Oda, M.Maeda, S.Hibi, Kobunshi Kagaku, 30, 337, 288-295, (1973)

SUMMARY

Scattering of various radiations on inhomogeneities in materials is a basis for a number of techniques that can be applied to studies of polymeric blends. Possible applications of methods basing on X-Ray, neutron or light scattering, to the investigation of the structure of blends are analysed. A spectrum of Structure levels, that might occur due to complex interactions between components, is reviewed and problems concerning appropriate choice of a technique are discussed.